

# Aerosol optical properties retrieved using Skyradiometer at Hanle in western Himalayas

Neeharika Verma, S.P. Bagare, Shantikumar Singh Ningombam\*, Rajendra B. Singh

Indian Institute of Astrophysics, Koramangala, Bangalore 560034, India

## ARTICLE INFO

### Article history:

Received 20 April 2009

Received in revised form

15 October 2009

Accepted 24 October 2009

Available online 6 November 2009

### PACS:

01.30. – y

### Keywords:

Aerosol optical depth

Single scattering albedo

Volume size distribution

Refractive indices

## ABSTRACT

A Skyradiometer was installed at Hanle in Ladakh, in October 2007 as a part of the site characterization program for the proposed National Large Solar Telescope project. Aerosol optical depth (AOD), single scattering albedo (SSA), volume size distribution, and refractive indices were retrieved at five spectral channels, using measurements of direct and diffuse solar irradiation. At 500 nm, the yearly average values of AOD and SSA were found to be 0.05 and 0.965, respectively. The volume size distribution shows a general bimodal behavior with two peaks at around 7–10 and 0.1–0.2  $\mu\text{m}$  with an occasional tri-modal behavior.

© 2009 Elsevier Ltd. All rights reserved.

## 1. Introduction

Natural and anthropogenic activities induce minute particles in the terrestrial atmosphere. These particles, called aerosols, remain suspended in the atmosphere for a significant period of time, days to weeks. Their volume and size distributions vary spatially and temporally depending upon the changes in the atmospheric conditions such as wind (Peterson et al., 1981; Hoppel et al., 1990), precipitation (Flossmann et al., 1985) and convective activity (Pueschel et al., 1972). Aerosols are transported both over short and long distances, controlled mainly by the thermal and dynamical effects in the atmosphere. Aerosols are mainly located near the boundary layer and their number concentrations depend on topographical locations, atmospheric conditions, annual and diurnal cycles and local sources. Usually, higher concentrations are found in urban and industrial areas while they are minimal in high altitude locations. In desert areas, aerosols are larger in size and depending upon their chemical composition, their light scattering efficiency and refractive index changes. As the particle size grows, particle scattering efficiency increases, and consequently single spectral albedo (SSA) also changes. The retrieval of SSA is sensitive to both the real and

imaginary parts of the refractive index. There is a limited information available about the particle sizes and aerosols types from their spectral dependence of aerosol optical depth (AOD) through their size distribution. But it is difficult to infer the detailed chemical composition from aerosol optical depth. Particles in the size range of 0.1–1.0  $\mu\text{m}$  are most important in producing radiative and optical effects, which in turn play a major role in cloud microphysical processes and visibility in the atmosphere. Scattering of solar radiation by aerosols, which is referred to as turbidity of the atmosphere (Iqbal, 1983), is a function of both number and size distribution of aerosols. In addition to various studies of aerosol properties, aerosol radiative forcing remains one of the largest uncertainties in the current assessment and prediction of global climatic changes (IPCC, 2001).

Further, radiation from celestial sources reaching the terrestrial atmosphere are affected by aerosols, thus limiting the performance of the ground based astronomical telescopes. Therefore, detailed analysis of aerosol content provides one of the inputs necessary for the selection of a good astronomical site. The Indian Astronomical Observatory (IAO) is located at Hanle which is a high altitude site having typical features of a cold-desert and very dry atmospheric conditions. In addition, the near absence of anthropogenic activity in the region results in very low aerosol content at the site. The Indian Institute of Astrophysics is presently operating a 2 m Himalayan Chandra Telescope (HCT) at Hanle. The Institute is further looking for a suitable site to

\* Corresponding author. Tel.: +91 80 2553 0672; fax: +91 80 2553 4043.  
E-mail address: shanti@iiap.res.in (S.S. Ningombam).

locate the proposed National Large Solar Telescope (NLST) in the western Himalayas and the surrounding region. Hanle and two other sites in the region have been selected for detailed site characterization. In this context, several instruments were installed at Hanle during the year 2007, including a Skyradiometer (POM-01L from M/s Prede, Japan) which was installed in the month of October. Preliminary results obtained from this instrument are presented in this study.

## 2. Description of the site

Hanle is located at  $32^{\circ}47'N$  and  $78^{\circ}58'E$  with an altitude of 4500 m. It has a minimal precipitation of  $<10$  cm in a year. Monthly averaged meteorological parameters such as temperature, relative humidity, and wind speed during 2007–2008 are presented in this paper. The monthly averaged data are evaluated from the five secondly measured automatic weather station data, which is used for the observational purpose of 2-m Himalayan Chandra Telescope. Day and night data are separated according to morning–evening and evening–morning twilight hours, respectively. It is found that the monthly averaged day and night temperature during summer months (July–August) is ranging in between  $9$  and  $14^{\circ}C$  and where as in winter (January–February) it ranges in between  $-8$  and  $-14^{\circ}C$ , as seen in Fig. 1(a). The site is significantly dry throughout the year with the averaged monthly relative humidity at 28.1% and 35.2%, during day and nights, respectively, as seen in Fig. 1(b). The monthly averaged day-time wind speed in the summer and winter months are around 5 and

$6.0 \text{ ms}^{-1}$ , respectively, displaying marginal seasonal differences as seen in Fig. 1(c). However, the winds follow a general pattern at the site, starting with a mild wind at the early hours of the day, picking up gradually and reaching the peak values of up to  $15\text{--}20 \text{ ms}^{-1}$  in the afternoon. The prevailing wind direction is predominantly south westerly as shown in Fig. 2. The wind speed reduces significantly by evening and remains relatively low throughout the night and till early in the morning. Fig. 2 shows polar plots for the surface wind speed and direction, for both day and night time, from January 2007 to December 2008.

## 3. Instrumentation

The Skyradiometer consists of an automatic sun tracking system, a spectral scanning radiometer, a rain detector, and a sun sensor. The unique features of the instrument include, an in-built calibration capability, an automatic solar disk scanner for calibration of solid view angle, and a single detector design. It has seven filters with central wavelengths at 315, 400, 500, 675, 870, 940 and 1020 nm with band widths ranging from 2 to 10 nm. The instrument measures solar irradiance, both direct and diffuse, in almucantar as well as principle plane geometry. In the data analysis, 315 and 940 nm measurements were excluded due to peak ozone and water vapor absorption at the respective wavelengths. The direct solar irradiance is measured for every 20 min, or 0.25 steps in air mass. The diffuse solar irradiance is measured for every 1 min interval. The aerosol optical properties such as aerosol optical depth (AOD), single scattering albedo

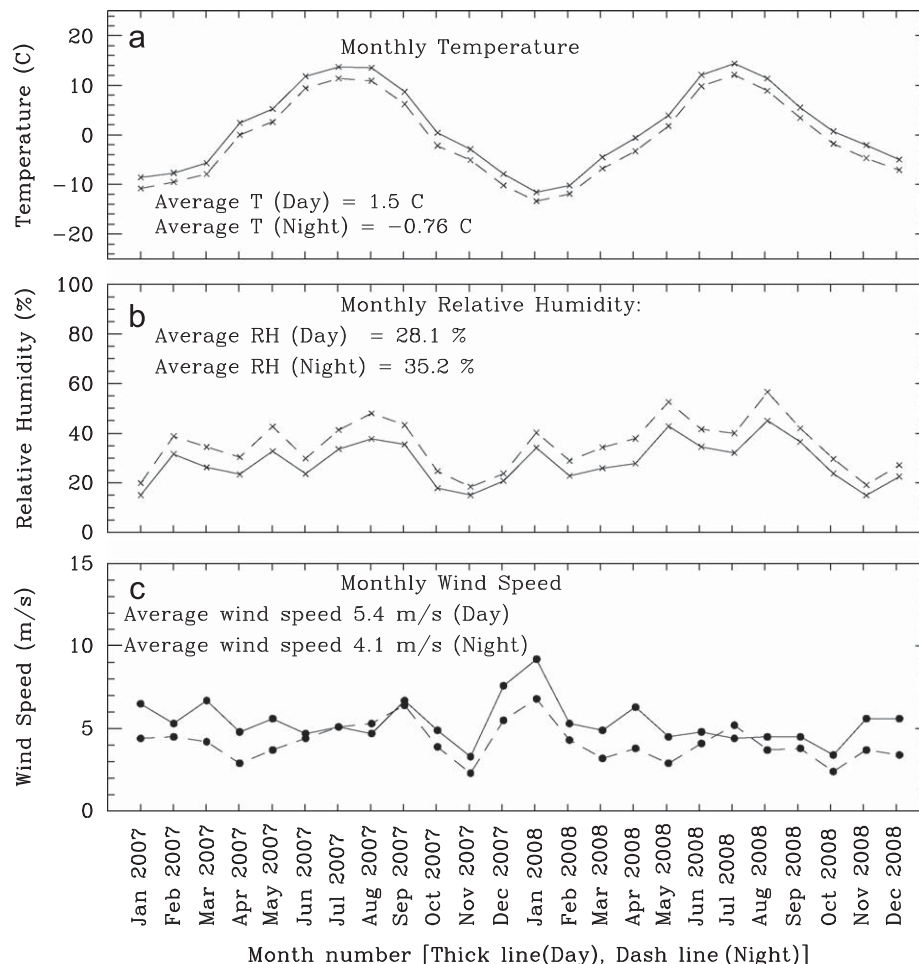


Fig. 1. Monthly average variation of (a) air temperature (b) relative humidity, and (c) surface wind speed at Hanle during 2007–2008.

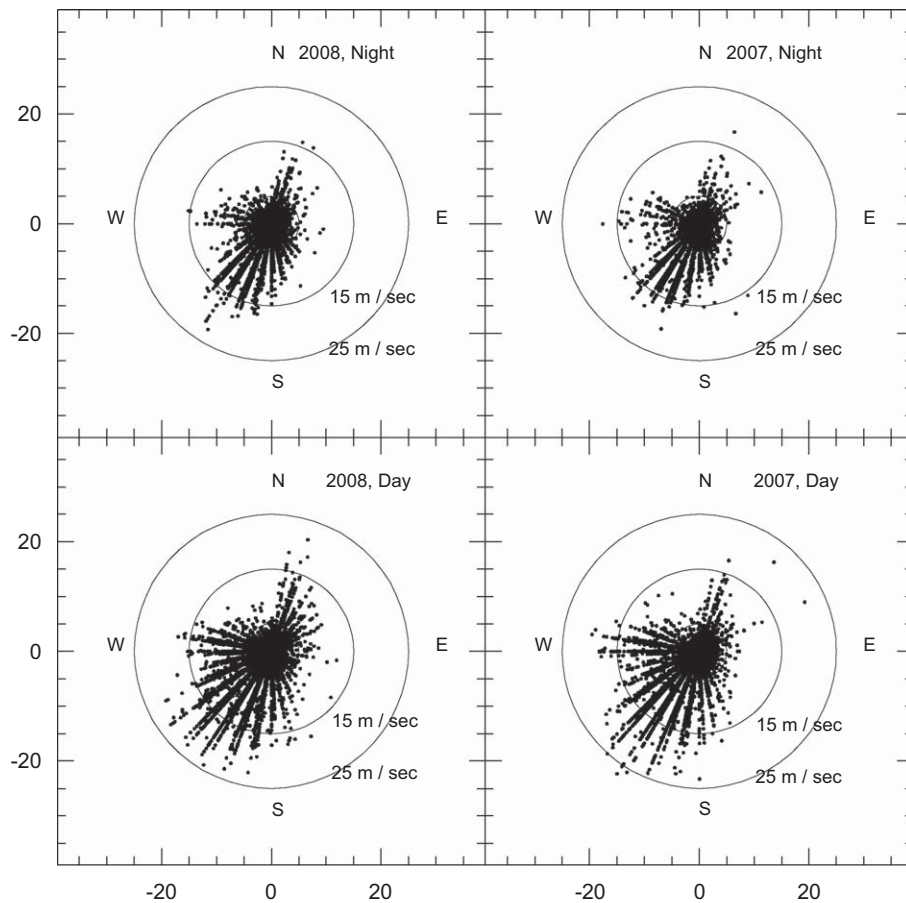


Fig. 2. Surface wind speed and wind direction during day and night time at Hanle for the period January 2007 to December 2008.

Table 1

Results of solid view angles (in Steradian) determined from disk scan data during selected observing period.

Dates	400 nm	500 nm	675 nm	870 nm	1020 nm
10/10/07	2.450E−4	2.460E−4	2.440E−4	2.496E−4	2.510E−4
10/09/08	2.460E−4	2.470E−4	2.470E−4	2.490E−4	2.490E−4
29/09/08	2.440E−4	2.450E−4	2.450E−4	2.480E−4	2.520E−4
30/09/08	2.440E−4	2.440E−4	2.450E−4	2.480E−4	2.490E−4
01/10/08	2.450E−4	2.460E−4	2.440E−4	2.460E−4	2.510E−4
02/10/08	2.440E−4	2.450E−4	2.460E−4	2.500E−4	2.510E−4
03/10/08	2.440E−4	2.480E−4	2.450E−4	2.500E−4	2.510E−4
04/10/08	2.440E−4	2.440E−4	2.430E−4	2.490E−4	2.530E−4

(SSA), phase functions and volume size distribution are derived from the measured sun/sky irradiance data for the five spectral bands by using Skyrad.Pack (version 4.2) as described in Nakajima et al. (1996).

### 3.1. Calibration of the Skyradiometer

Calibration of instruments is very essential for obtaining reliable data. In many of the instruments used at field experiments, filters deteriorate in course of time, resulting in a gradual decrease of percentage transmission and a shift of the central wavelength. Such degradation of filter may occur due to moisture or excessive exposure to intense heat radiation during field

observations. Usually, calibration of ground based instruments are performed at high altitude, in pristine mountain tops, where the aerosol concentration and atmospheric turbulence are minimal.

The Skyradiometer has provision for auto disk scan to measure the solid view angle for each channel. Disk scan is performed in an area of  $2^\circ \times 2^\circ$  around the solar disk with an angular resolution of  $0.1^\circ$ . In general, the radiometer is operated once in a month in disc scan mode to estimate solid view angles for different channels. Table 1 presents the results for a few select days having fully clear sky conditions. The results of the solid view angle of each channel of the instrument is nearly stable with  $< 0.5\%$  deviation from the values given by PREDE at the time of installation. The difference of AOD due to such a small variation in solid view angle is almost negligible. Besides, the improved Langley method of calibration

was regularly carried out for clear days data having low atmospheric turbulence using the Skyrad.pack software. The main uncertainties in retrieving AODs is due to improper values of calibration constants (FOs). In the present work, calibration constants obtained on select clear sky days are studied for various aspects such as seasonal and monthly variations. During the one year period of study, calibration constant obtained through the improved Langley method shows a relative standard deviation (RSD) of 5.8%, 4.7%, 4.4%, 5.0% and 3.9% at 400, 500, 675, 870 and 1020 nm, respectively. The results obtained at Hanle show similar pattern as discussed by Xia et al. (2004). It is further noticed that 1% change in FOs corresponds to  $\sim 0.01$  change in the derived AOD. Since AOD measured at such a high altitude location is very small unlike in other urban locations, it is very essential to calculate optical depth due to Rayleigh factor accurately. The optical depth due to Rayleigh scattering at each of the filters was corrected using the monthly averaged station pressure. The maximum and minimum pressure difference at Hanle is around 1% of the daily mean. The difference of AOD due to 2% variation in station pressure is around 0.004–0.002 at 400 and 500 nm, respectively, and rest of the filters show negligibly small values. It is found that both normal and modified Langley plots are in good agreement at shorter wavelengths (400, 500, and 675 nm) but notable deviation is observed at longer wavelengths (870 and 1020 nm), apparently arising from aerosol absorption. Fig. 3 shows the normal Langley plot taken on 12 October 2008 for illustration. The forenoon and afternoon data points show similar behavior with a marginal departure for the higher wavelength bands.

Fig. 4(a–d) shows the correlation between measured and retrieved AOD values obtained for 400, 500, 675, and 1020 nm, respectively, for the period October 2007 to December 2008. The measured AOD values were obtained from the direct data using the calibration constant, whereas the retrieved AOD were obtained using both direct and diffuse solar irradiation. The performance of the Skyradiometer was routinely checked with the assistance of M/s Prede of Japan.

## 4. Results and discussion

### 4.1. Aerosol optical depth

#### 4.1.1. Seasonal and diurnal variation

The retrieved values for AOD at Hanle are generally very low throughout the year. The annual average observed at 500 nm during the period October 2007 to October 2008 was  $0.050 \pm 0.001$ . The frequency of occurrence vs AOD are plotted in Fig. 5(a) for all days of the one year period, (b) for the summer months of April to September, and (c) for the winter months of October to March, respectively. A seasonal variation is evident with the peaks of AOD values occurring in the range of 0.03–0.05 during summer and 0.02–0.04 during the winter months.

Fig. 6 shows the diurnal variation of AOD on typical summer and winter clear days for five channels. During summer, the increase in AOD may occur due to increase in convective activity arising from the dry ground surface combined with strong surface winds. During winter, a minimal AOD is observed as expected due to low convective activity caused by much cooler ground surface.

On some occasions, higher AOD values of above 0.1 were observed, but such cases are rather rare. It is suspected that such high values of AOD might be due to the combination of wind blown desert dust from dry land surface as well as the desert dust reaching at the site through long range transport phenomenon. It is likely that the phenomenon might be triggered by the prevailing south-westerly winds with speed of more than  $15 \text{ ms}^{-1}$ . It may be mentioned that the Thar and Sahara deserts are located in the south western direction of Hanle.

The observed values of AOD at Hanle are comparable to those reported from other high altitude continental sites. An annual mean AOD value of 0.05 at 500 nm is reported by Cong et al. (2009) at their AERONET (Aerosol Robotic Network) station, Nam Co (4720 m amsl), located in central Tibetan Plateau. Similarly, annual average AOD at 500 nm for the high altitude pristine mountain top of Mauna Loa (3400 m amsl) is reported as 0.02, with a seasonal peak of 0.033 during February–March (Holben

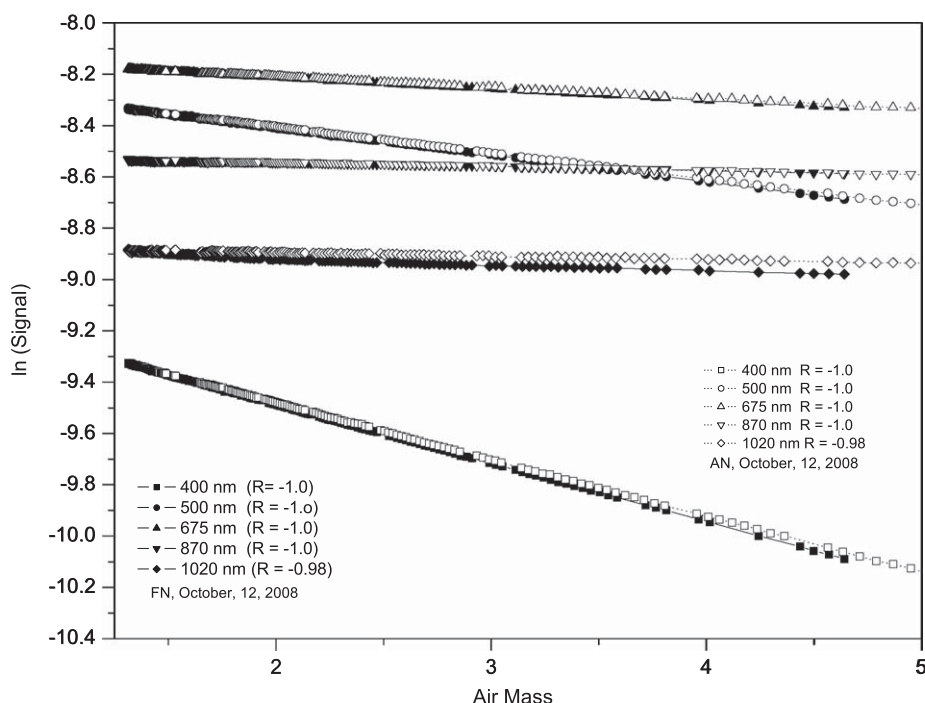
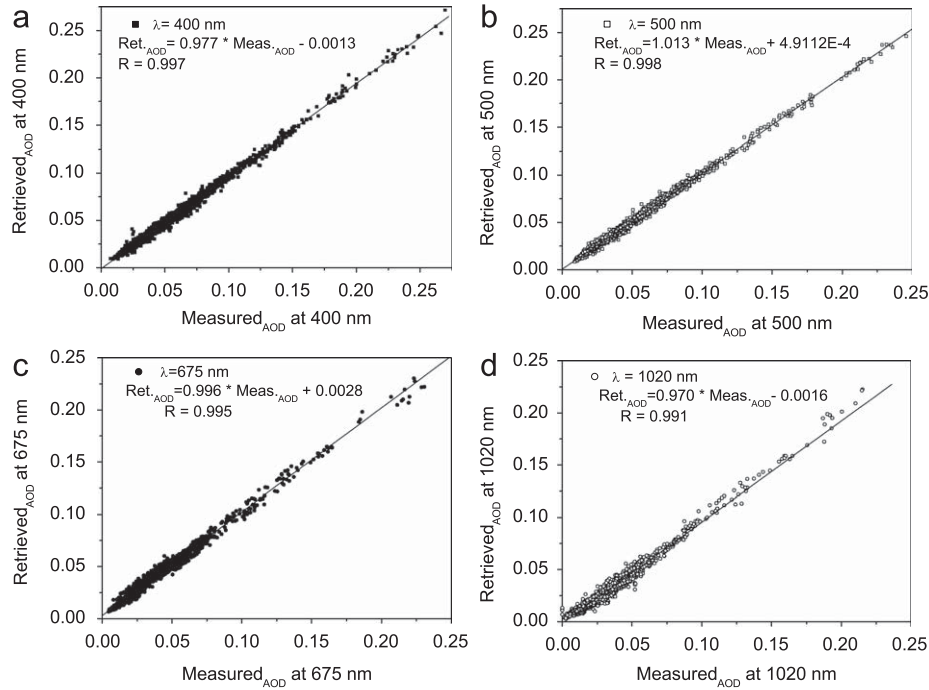
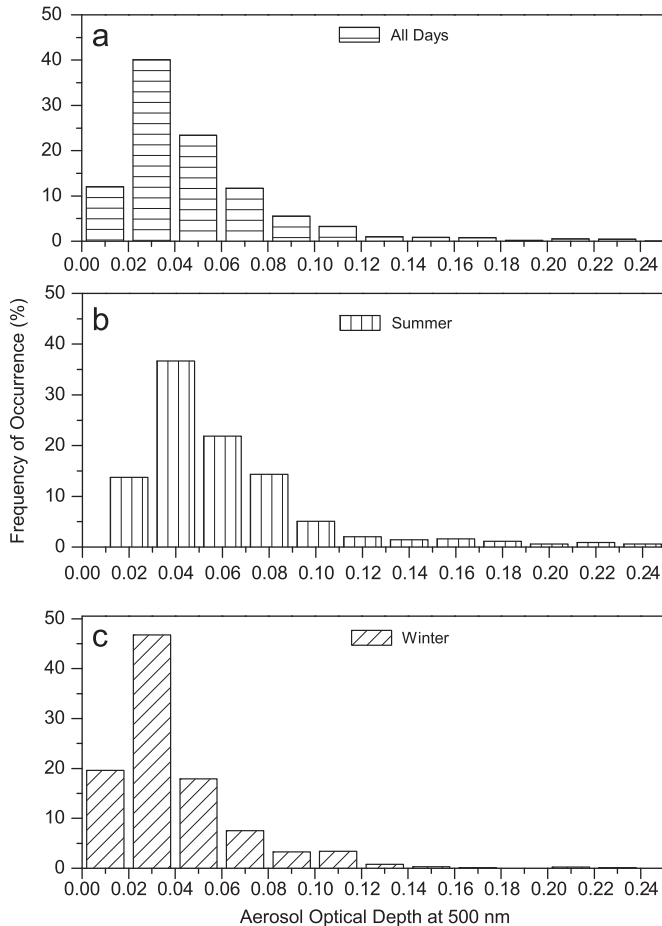


Fig. 3. Langley plot for a typical clear day (12 October 2008). The forenoon (FN) and afternoon (AN) parts are plotted separately.



**Fig. 4.** Scatter diagram of measured vs retrieved AOD for the five wavelengths (a) 400, (b) 500, (c) 675, and (d) 1020 nm, corresponding to the period from October 2007 to October 2008.



**Fig. 5.** Percentage frequency distribution of AOD at 500 nm obtained for October 2007 to October 2008.

et al., 2001). It also turns out that the low AOD values of Hanle are comparable with those observed in the cold climatic conditions of polar regions. Six et al. (2005) have reported AOD as low as 0.02 for 440 nm at Dome C in Antarctica.

#### 4.1.2. Angstrom's exponent

The aerosol optical depth,  $\tau_a(\lambda)$  is related to the atmospheric turbidity coefficient,  $\beta$  as follows:  $\tau_a(\lambda) = \beta \lambda^{-\alpha}$ , where  $\alpha$  is the Angstrom's (1961) exponent, and  $\lambda$  is the wavelength in  $\mu\text{m}$ . The parameter,  $\beta$  or turbidity coefficient, indicates the aerosol concentration, while the Angstrom's exponent,  $\alpha$  is related to its size distribution. The larger values of  $\alpha$  indicate a relatively high ratio of small to large particles. It is expected that when the aerosol particles are very small,  $\alpha$  may go up to 4 and is nearly 0 for the large size particles. The parameters  $\alpha$  and  $\beta$  are determined by taking log-log scale of the above relation, using the measured AODs at 400, 500, 675, and 870 nm.

In the present work, an attempt was made to study the behavior of  $\alpha$  with the instantaneous surface wind speed. The observing site has relatively higher wind speed and in the case of a windy day, it starts with a mild wind at the early hours of the day, picking up gradually and reaching the peak values of up to  $15\text{--}20\text{ ms}^{-1}$  in the afternoon. The monthly averaged wind speed at the observing site is around  $5\text{--}6\text{ ms}^{-1}$ . It is expected that both fine and coarse mode particles are injected into the atmosphere by the action of strong surface wind speed from the dry land mass. Fig. 7(a and b) shows the results of nearly two consecutive days observations in two typical windy days; 26, and 29 in October 2007. In Fig. 7(a),  $\alpha$  varies from 1.2 to 0.3 with the corresponding wind speed from 0 to  $13\text{ ms}^{-1}$ . In Fig. 7(b),  $\alpha$  varies from 0.8 to 0.2 with the corresponding wind speed from 0 to  $17\text{ ms}^{-1}$ . Fig. 7(c) shows relatively lesser wind speed than Fig. 7(a and b), with the higher  $\alpha$  (fine mode aerosols) values. It suggested that there is presence of both coarse and fine mode aerosols at the site and the coarse mode aerosols are responsible



due to wind driven desert dust aerosols. The presence of both fine and coarse mode aerosols at Hanle is also indicated by the bi-modality nature of aerosol size distribution. Significant anti-correlations of  $-0.79$ ,  $-0.83$  and  $-0.85$ , respectively, were obtained between  $\alpha$  with the instantaneous surface wind speed as seen in Fig. 7(a–c) during the typical windy days of study. Similar results of significant anti-correlation between  $\alpha$  with instantaneous surface wind has been reported by Smirnov et al. (2003) at Midway Island in the central Pacific Ocean.

#### 4.1.3. Long range transport

In the case of long range transport of air pollutants, it is possible to trace their movement of air mass by using the low-altitude flow field computed from a meso-scale model. Wind field patterns computed using these models represent the dispersion of air pollutants (Fang et al., 1999). Interpretation for the influence of aerosol transport phenomenon is obtained using the back trajectory analysis of Hybrid Single Particle Lagrangian integrated Trajectory (HYSPLIT) model (Version 4), developed by Draxler and Rolph, at Air Resources Laboratory, NOAA. This analysis provides latitude-longitude distribution of kinematic wind field including horizontal and vertical wind velocities. In the present study, the back-trajectory analysis for Hanle has been carried out for two typical days, one each for summer and winter months. Figs. 8 and 9 show three days back trajectory analysis ending 0600 UT of 26 October 2007 and 30 April 2008, respectively, pertaining to 6000, 7000 and 8000 m above ground level (AGL) in the atmospheric air column. The observed higher values of AOD with the simultaneous study of back trajectory HYSPLIT model suggests the influx of desert aerosols (Saharan type) towards the observing station.

#### 4.2. Single scattering albedo

Single scattering albedo (SSA) is one of the parameters used in the determination of aerosol radiative forcing. It is defined as the

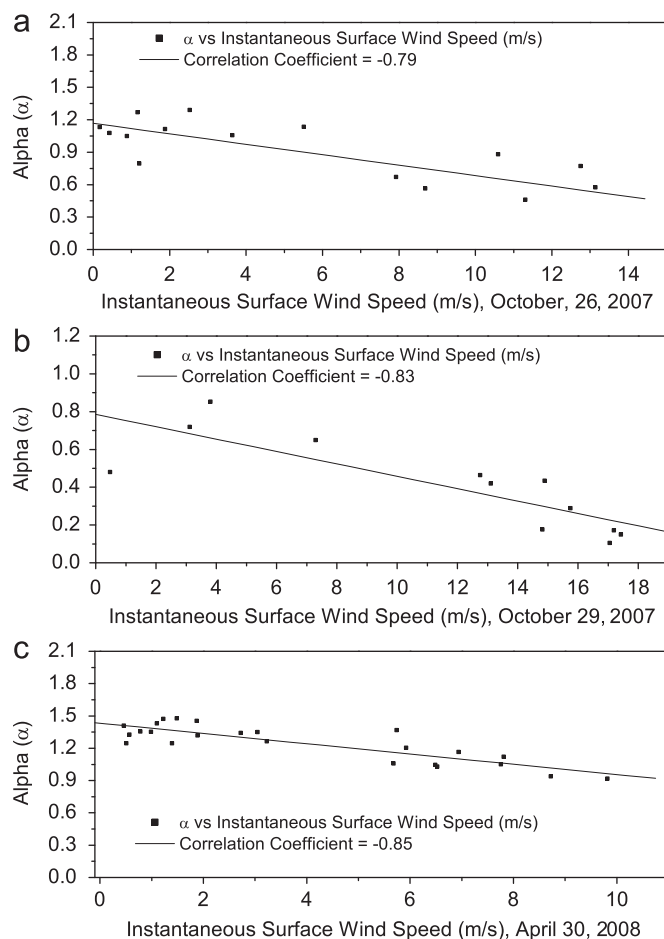


Fig. 7. Alpha vs instantaneous surface wind speed behavior for typical windy days of (a) and (b) in early winter, and (c) in summer period at Hanle.

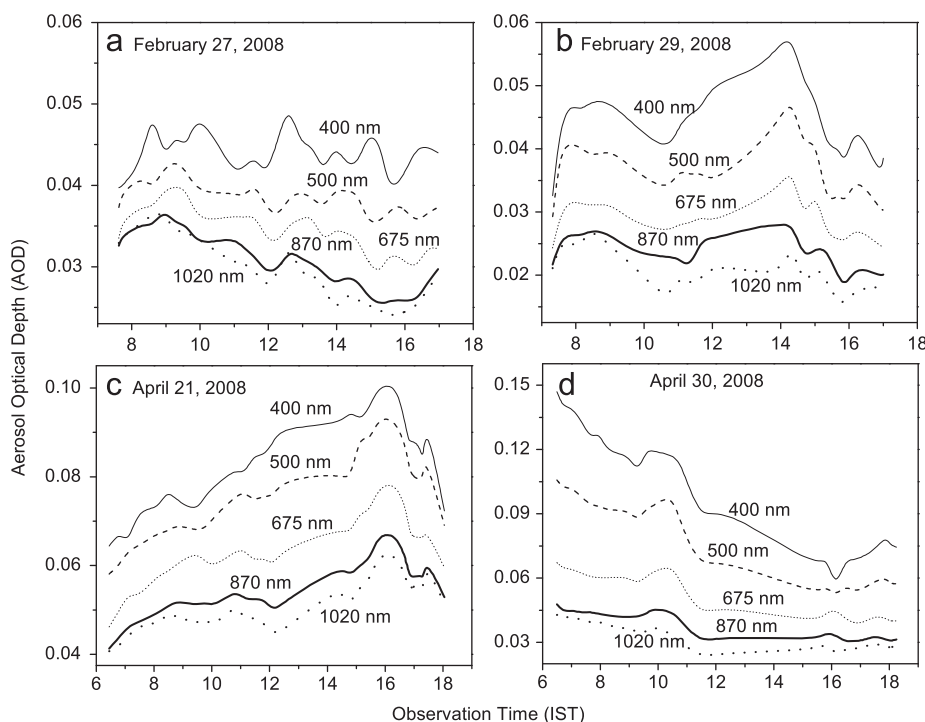


Fig. 6. Diurnal variation of AOD on two typical winter (a, b) and summer (c, d) days at Hanle.

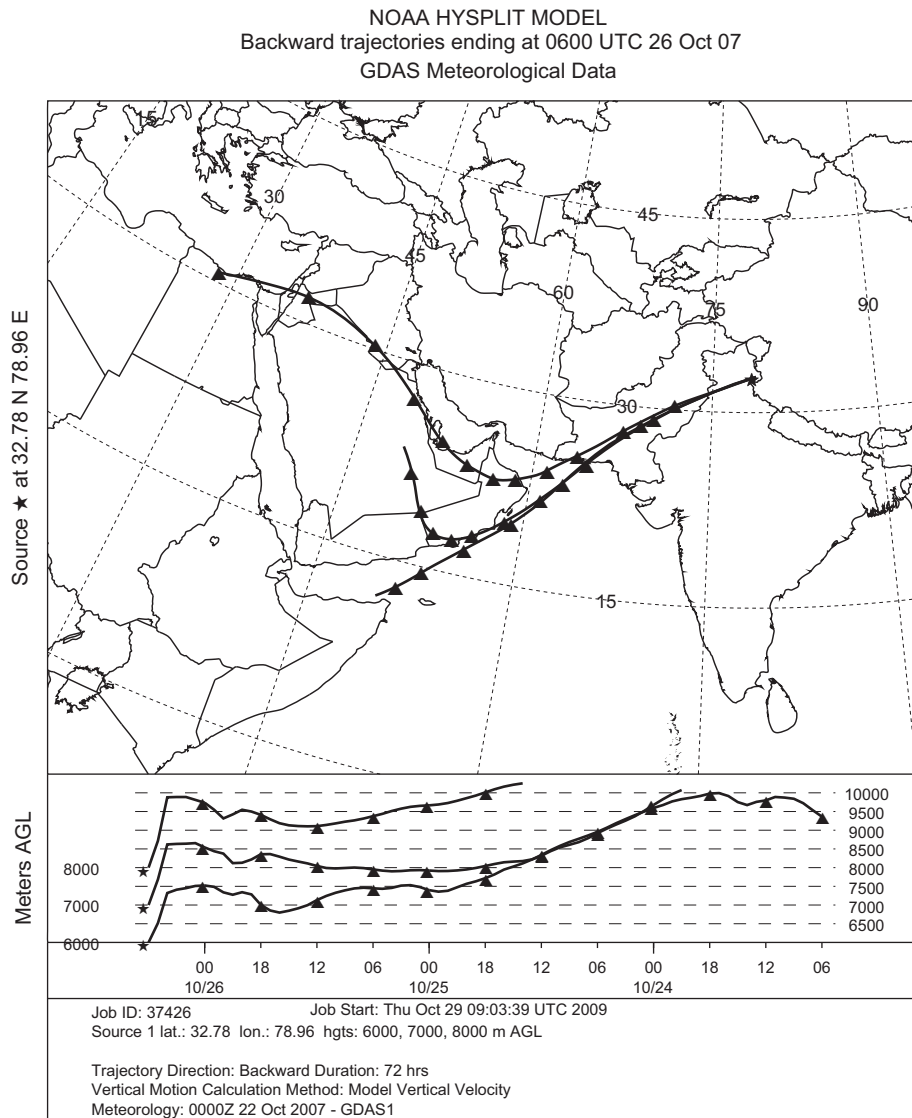


Fig. 8. The three days back trajectory HYSPLIT model, ending on a typical windy early winter day (26 October 2007) over Hanle.

ratio of scattering coefficient to the total extinction (scattering + absorption) coefficient. Its value ranges from 0 to 1 for totally absorbing and totally scattering aerosols, respectively. In view of its importance in climate forcing, extensive studies were carried out by many authors for the evaluation of SSA (Anderson et al., 1999; Devaux et al., 1998; Dubovik et al., 1998; Yu et al., 2000). Fig. 10 shows the daily mean of SSA obtained during the period of our observations. The observed high values of SSA during the entire period of study may indicate a strong presence of scattering aerosols such as silicates and sulfate particles. Earlier, Singh et al. (2005) have indicated the strong presence of non-absorbing aerosols in this high altitude region of Ladakh and Hanle. The mean values of SSA are  $0.96 \pm 0.002$  and  $0.97 \pm 0.002$  at 500 nm, during winter and summer seasons, respectively, as seen in Fig. 10(a). Pant et al. (2006) have reported the inferred SSA at the high altitude, Manora Peak in Central Himalayas in the range of 0.87–0.94. The SSA values obtained at Hanle are slightly higher than those at Manora peak. The desert dust origin with barren vast land mass of Hanle may be understood to result in the observed higher values of SSA.

Further, Fig. 11(b) shows the spectral variation of real and imaginary parts of refractive index, obtained during the period of

our study. The value of imaginary part of refractive index defines the magnitude of aerosol absorption. The physical and chemical composition of aerosols can be inferred from a detailed study of these results. It is seen from Fig. 11(a) that the SSA values show significant departure for low  $\lambda$  ( $< 500$  nm) and for high  $\lambda$  ( $> 800$  nm). This aspect is under investigation.

#### 4.3. Aerosol size distribution

Fig. 12 (a,b) shows the diurnal variation of aerosol columnar volume size distributions derived using Skyrad.pack, for two select days, one each in April and October months. A bi-modal distribution is evident with the higher peak at around  $10 \mu\text{m}$  and the lower peak around  $0.1 \mu\text{m}$ . However, in the summer month of April, a tri-modal size distribution emerges. Similar to our results, a tri-modal type of size distribution of aerosols has been reported by Che et al. (2007) from their Skyradiometer (Prede) measurements over Beijing. In our present study, there is an indication for the presence of both fine and coarse mode particles during the period of our study. The fine mode has a radius of  $0.10$ – $0.20 \mu\text{m}$  and the coarse mode has radius of

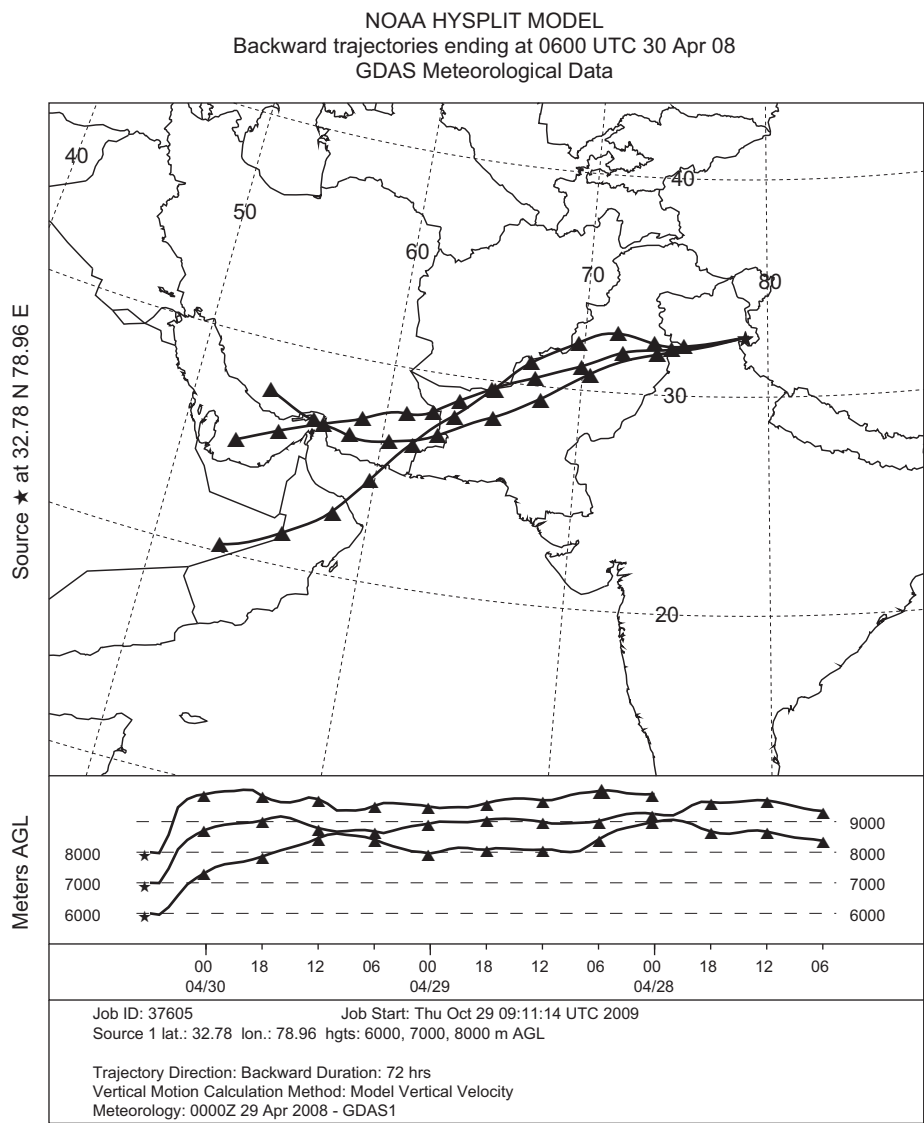


Fig. 9. The three days back trajectory HYSPLIT model, ending on typical windy early summer day (30 April 2008) over Hanle.

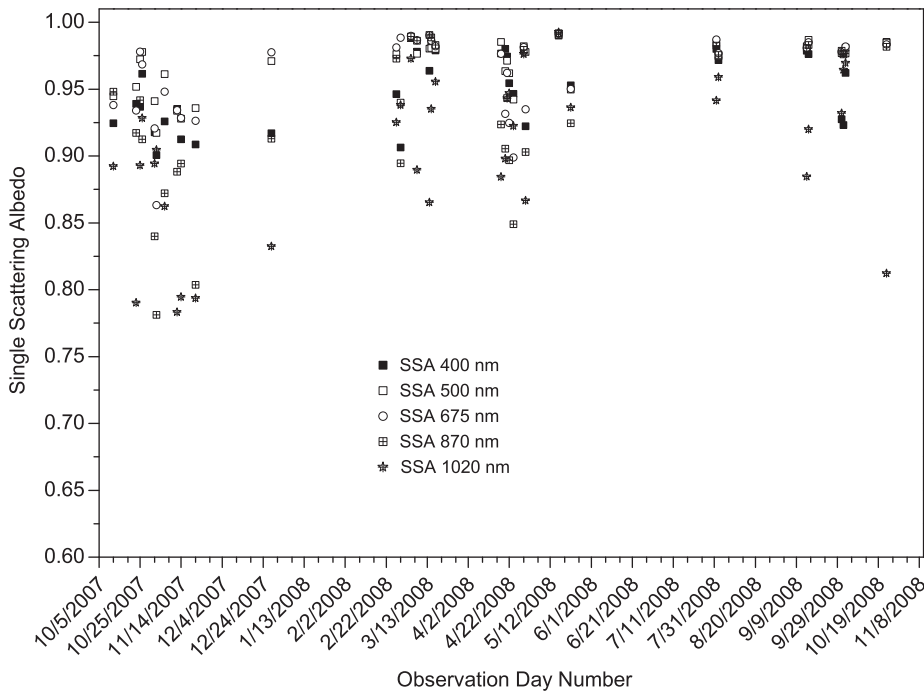
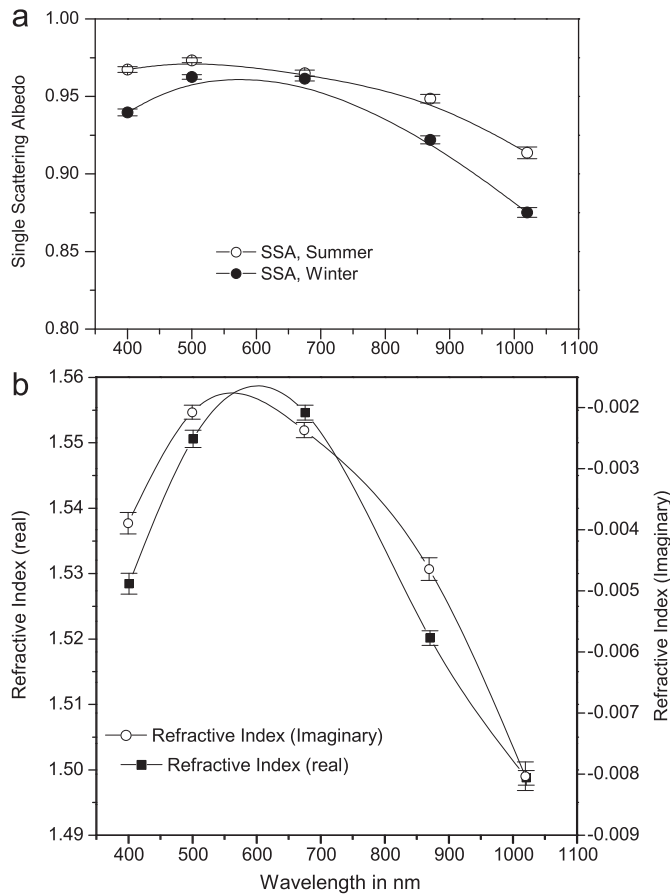


Fig. 10. Daily variation of single scattering albedo during the clear days of observation at Hanle.





**Fig. 11.** Seasonal variation of SSA and Refractive index (real and imaginary parts) during the entire period of study.

7–10  $\mu\text{m}$ . The presence of such large size (coarse mode) aerosols has been reported earlier by Cong et al. (2009) at their high altitude AERONET site, Nam Co, (4730 m), a remote site in central Tibetan Plateau. Further, Jain et al. (2007) have reported that with the increase in altitude, the mass concentration and the percentage of surface aerosols in fine mode decreases, whereas the proportion of coarse and large mode aerosols increases.

## 5. Conclusions

- (1) The daily AOD values obtained using Skyradiometer observations at Hanle are below the general background level. The yearly average AOD value at 500 nm is  $0.050 \pm 0.001$ , with maximum and minimum of  $0.063 \pm 0.002$  and  $0.040 \pm 0.001$ , during summer and winter months, respectively. The obtained aerosol optical properties at Hanle are comparable with those reported at other high altitude sites such as Nam Co, in central Tibetan Plateau.
- (2) On some occasions, higher AOD values of above 0.1 are observed, but such cases are rather rare. It is suspected that long range transport of dust aerosols contribute to higher AOD values at the observing station. This phenomenon may be triggered by the strong prevailing south westerly wind in the region.
- (3) Aerosol size parameter ( $\alpha$ ) shows significant anti-correlation with the heavier instantaneous surface wind speed, at the site. It is suggested that coarse mode aerosols are generated primarily due to wind driven desert dust aerosols.

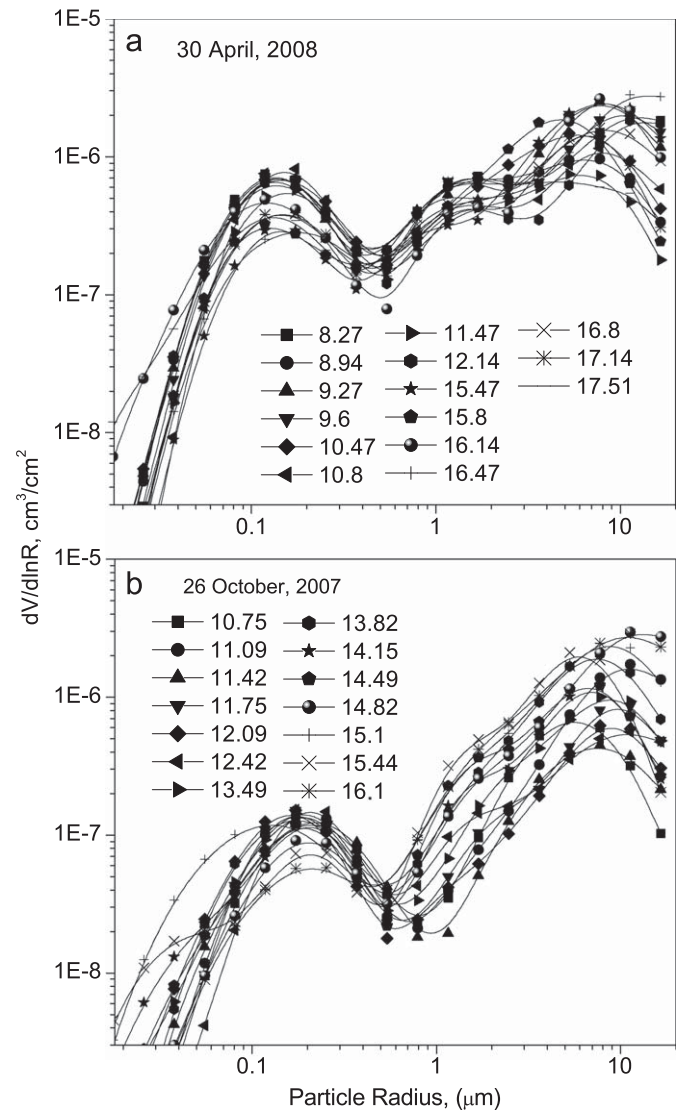


**Fig. 12.** Aerosol volume size distribution obtained on two typical days at Hanle during summer (a) and winter (b) periods of observation.

- (4) Back trajectories derived from the HYSPLIT model computations indicate the presence of parcel of air mass coming from the Saharan desert.
- (5) The inferred average values of SSA during winter and summer seasons are  $0.96 \pm 0.002$  and  $0.97 \pm 0.002$  at 500 nm, respectively. The higher values of SSA at Hanle indicate strong absence of absorbing aerosols such as those of anthropogenic origin.
- (6) The derived volume size distribution shows a general bimodality with the higher peak at around 7–10  $\mu\text{m}$  and the lower peak at around 0.1–0.2  $\mu\text{m}$  with an occasional trimodal trend, usually in the summer months. This result also suggests the presence of desert dust at the site.

## Acknowledgments

The authors would like to thank S.S. Hasan, Director (IIA) for support and encouragement. The entire staff of IAO-Hanle extended invaluable help during observations. The Skyradiometer data were analyzed using the Skyrad.pack software, version 4.2. The authors thank T. Nakajima, M. Yamano, and Kazuma Aoki for

related clarifications. Thanks are due to T.P. Prabhu, K.E. Rangarajan and K. Krishna Moorthy for valuable suggestions while preparing the manuscript. In addition, the authors are grateful to Chris A. Gueymard and Monica Campanelli, for useful discussions. The HYSPLIT back-trajectories analysis in this work was carried out using the FNL archived data at the NOAA, Air Resources Laboratory.

## References

- Anderson, T.L., Covert, D.S., Wheeler, J.D., Harris, J.M., Perry, K.D., Trost, B.E., Jaffe, D.J., Ogren, J.A., 1999. Aerosol backscatter fraction and single scattering albedo: measured values and uncertainties at a coastal station in the Pacific Northwest. *J. Geophys. Res.* 104, 26793–26807.
- Angstrom, A., 1961. Techniques of determining the turbidity of the atmosphere. *Tellus* 13, 214–223.
- Che, H., Shi, G., Uchiyama, A., Yamazaki, A., Chen, H., Goloub, P., Zhang, X., 2007. Intercomparison between aerosol optical properties by a Prede Skyradiometer and CIMEL Sunphotometer over Beijing, China. *Atmos. Chem. Phys.* 8, 3199–3214.
- Cong, Z., Shichang, K., Alexander, S., Brent, H., 2009. Aerosol optical properties at Nam Co, a remote site in central Tibetan Plateau. *Atmos. Res.* 92, 42–48.
- Devaux, C., Verneulen, A., Deuze, J.L., Dubuisson, P., Herman, M., Santer, R., Verbrugghe, M., 1998. Retrieval of aerosol single-scattering albedo from ground-based measurements: Application to observational data. *J. Geophys. Res.* 103, 8753–8761.
- Dubovik, O., Holben, B.N., Kaufman, Y.J., Yamasoe, M., Smirnov, A., Tanre, D., Slutsker, I., 1998. Single-scattering albedo of smoke retrieved from the sky radiance and solar transmittance measured from ground. *J. Geophys. Res.* 103, 31,901–31,923.
- Fang, M., Zheng, M., Wang, F., Chim, K.S., Kot, S.C., 1999. The long-range transport of aerosols from northern China to Hong Kong—a multi-technique study. *Atmos. Environ.* 33, 1803–1817.
- Flossmann, A.I., Hall, W.D., Pruppacher, H.R., 1985. A theoretical study of the wet removal of atmospheric pollutants, part I: the redistribution of aerosol particles captured through nucleation and impaction scavenging. *J. Atmos. Sci.* 42, 583–606.
- Holben, B.N., Tanr, D., Smirnov, A., Eck, T.F., et al., 2001. An emerging ground-based aerosol climatology: aerosol optical depth from AERONET. *J. Geophys. Res. Atmos.* 106, 12067–12097 and 19 coauthors.
- Hoppel, W.A., Fitzgerald, J.W., Frick, G.M., Larson, R.E., Mack, E.J., 1990. Aerosol size distributions and optical properties found in the marine boundary layer over the Atlantic Ocean. *J. Geophys. Res.* 95, 3659–3686.
- Iqbal, M., 1983. *An Introduction to Solar Radiation*. Academic Press, Toronto.
- International Panel on Climate Change, 2001. *The Scientific Basis*. Cambridge University Press, New York.
- Jain, S.L., Kulkarni, P.S., Arya, B.C., Kumar, A., Ghude, S.D., Singh, P., 2007. Altitudinal variation of surface aerosol with change in site: a comparative study. *Ind. J. Radio Space Phys.* 36, 571–575.
- Nakajima, T., Tonna, G., Rao, R., Boi, P., Kaufman, Y., Holben, B.N., 1996. Use of sky brightness measurements from ground for remote sensing of particulate polydispersions. *Appl. Opt.* 35, 2672–2786.
- Pant, P., Hegde, P., Dumka, U.C., Sagar, R., Satheesh, S.K., Moorthy, K.K., Saha, A., Srivastava, M.K., 2006. Aerosol characteristics at a high-altitude location in central Himalayas: Optical properties and radiative forcing. *J. Geophys. Res.* 111, D17206, doi:10.1029/2005JD006768.
- Peterson, J.T., Flowers, E.C., Berri, C.J., Reynold, C.L., Rudisill, J.H., 1981. Atmospheric turbidity over central North Carolina. *J. Appl. Meteorol.* 20, 229–241.
- Pueschel, R.F., Machta, L., Cotton, F.G., Flower, E.C., Peterson, J.T., 1972. Normal incidence radiation trends on Mauna Loa, Hawaii. *Nature* 204, 545–547.
- Singh, S., Nath, S., Kohli, R., Singh, R., 2005. Aerosols over Delhi during pre-monsoon months: characteristics and effects on surface radiation forcing. *Geophys. Res. Lett.* 32, L13808, doi:10.1029/2005GL023062.
- Six, D., Fily, M., Blarel, L., Goloub, P., 2005. First aerosol optical thickness measurements at Dome C (East Antarctica), summer season 2003–2004. *Atmos. Environ.* 39, 5041–5050.
- Smirnov, A., Holben, B.N., Eck, T.F., Dubovik, O., Slutsker, I., 2003. Effect of wind speed on columnar aerosol optical properties at Midway Island. *J. Geophys. Res.* 108 (D24), 4802 doi:10.1029/2003JD003879.
- Xia Xiangao, Chen Hongbin, Wang Pucai, 2004. Aerosol properties in a Chinese semiarid region. *Atmos. Environ.* 38, 4571–4581.
- Yu, S., Saxena, V.K., Wenny, B.N., DeLuisi, J.J., Yue, G.K., Petropavlovskikh, I.V., 2000. A study of the aerosol radiative properties needed to compute direct aerosol forcing in the southeastern United States. *J. Geophys. Res.* 105, 24739–24749.